

# Effect of impurities on quasi-2D quantum antiferromagnet

A. L. Chernyshev<sup>1,†</sup>, Y. C. Chen<sup>2</sup>, and A. H. Castro Neto<sup>3,\*</sup>

<sup>1</sup>*Solid State Division, Oak Ridge National Laboratory, Oak Ridge, Tennessee 37831*

<sup>2</sup>*Department of Physics, University of California, Riverside, California 92521*

<sup>3</sup>*Department of Physics, Boston University, Boston, MA 02215*

(October 25, 2018)

We have studied the static and dynamic properties of quasi-two-dimensional quantum antiferromagnets (AF) diluted with spinless impurities using spin-wave theory and  $T$ -matrix approximation. We show that the spectrum of a 2D AF at long wavelengths is overdamped at arbitrary concentration of spinless impurities. The scattering leads to a new length scale  $\ell/a \sim e^{\pi/4x}$ ,  $x$  being impurity concentration and  $a$  the lattice spacing, beyond which the influence of impurities on the spectrum is dominant. Although the dynamical properties are significantly modified we show that 2D is not the lower critical dimension for this problem. Thus, in low-dimensional systems with disorder the connection between static and dynamic quantities is not straightforward. Our results are in quantitative agreement with the recent Monte Carlo simulations and experimental data for  $S = 1/2$ ,  $S = 1$ , and  $S = 5/2$ . We have also proposed experiments which can further test the results of our theory.

PACS numbers: 75.10.-b, 75.10.Jm, 75.10.Nr, 75.40.Gb

## I. INTRODUCTION

The discovery of superconducting cuprates has attracted much attention to the properties of diluted 2D, QHAF [1–10], the subject intensively studied some 30 years ago in the context of magnetism in diluted magnetic alloys [11,12]. Traditional view of the effect of local disorder on the spectrum of an ordered 3D antiferromagnet is that at long wavelengths the *form* of the spectrum is not modified. The only effects are the reduction of hydrodynamic parameters and a weak damping.

In this work we study the problem of impurities in 2D QHAF within the linear spin-wave theory using the  $T$ -matrix approach. The spin-wave Green's function is evaluated by summing all multiple-scattering diagrams that involve single impurity. We find that the scattering leads to a new length scale  $\ell/a \sim e^{\pi/4x}$  beyond which the influence of impurities on the spectrum is dominant. We associate this length scale with the localization length of spin excitations. We show that the dynamical structure factor  $\mathcal{S}(\mathbf{k}, \omega)$  for  $a^{-1} \gg k \gg \ell^{-1}$  consists of three parts (we use units  $\hbar = k_B = 1$ ): (i) a broadened quasiparticle peak with a width given by  $\Gamma_k \simeq x c_0 k$ ,  $c_0 = 2\sqrt{2}SJa$ ; (ii) a non-Lorentian localization peak at  $\omega = \omega_0 \sim c_0 \ell^{-1}$ , (iii) a flat background of states between  $\omega = c_0 k$  and  $\omega = \omega_0$ . Thus for every  $\mathbf{k}$ -state some weight is spread from the high energies to the low energies. For  $k \lesssim \ell^{-1}$  the quasiparticle and localization peaks merge into a broad incoherent peak that disperses in momentum space. We calculate the static magnetic properties and find a quantitative agreement with both MC simulations and experimental data. We show that at  $T = 0$  the staggered magnetization is given by  $M(x, 0) \approx S - \Delta - Bx$ , the factor  $\Delta \approx 0.2$  is the contribution of the zero-point fluctuations of the spins and  $B \simeq 0.21$ . We find that  $T_N(x)/T_N(0) \simeq 1 - A_s x$  where  $A_s = \pi - 2/\pi + B/(S - \Delta)$ . This result gives  $A_{1/2} \simeq 3.2$  and  $A_{5/2} \simeq 2.6$  which agree

very well with experiments up to  $x \simeq 0.25$ .

The systems discussed in this paper are modeled by the site-diluted quantum Heisenberg antiferromagnet:

$$H = \sum_{\langle ij \rangle} J_{ij} p_i p_j \mathbf{S}_i \cdot \mathbf{S}_j, \quad (1)$$

where  $p_i = 1$  (0) if  $i$ 's site is occupied (unoccupied) by the spin  $S$ . We focus on the problem of tetragonal or square lattices with in-plane,  $J$ , and out-of-plane,  $J_\perp$ , nearest-neighbor exchange constants,  $\langle ij \rangle$  denotes summation over bonds. In the systems of interest  $J \gg J_\perp$ . We begin with the Hamiltonian (1) in the linear spin-wave approximation which is split into the pure host and impurity part and, after the Bogolyubov transformation, is given by (in the units of  $4SJ$ )

$$\mathcal{H}_0 = \sum_{\mathbf{k}} \omega_{\mathbf{k}} \left( \alpha_{\mathbf{k}}^\dagger \alpha_{\mathbf{k}} + \beta_{\mathbf{k}}^\dagger \beta_{\mathbf{k}} \right), \quad (2)$$

$$\mathcal{H}_{imp} = - \sum_{l, \mathbf{k}, \mathbf{k}'} e^{i(\mathbf{k}-\mathbf{k}')\mathbf{R}_l} \hat{A}_{\mathbf{k}}^\dagger \hat{\mathcal{V}}_{\mathbf{k}, \mathbf{k}'}^l \hat{A}_{\mathbf{k}'}, \quad (3)$$

with two-component vectors  $\hat{A}_{\mathbf{k}}^\dagger = \left[ \alpha_{\mathbf{k}}^\dagger, \beta_{-\mathbf{k}} \right]$  and  $2 \times 2$  scattering potential matrices  $\hat{\mathcal{V}}_{\mathbf{k}, \mathbf{k}'}$  (for details see [14]),  $l$  runs over the impurity sites. We are interested in the Green's function of the Hamiltonian (2) modified by random impurity potentials (3). The Green's function is a  $2 \times 2$  matrix defined in a standard way and the  $T$ -matrix equation for the Hamiltonian (3) is given by:  $\hat{T}_{\mathbf{k}, \mathbf{k}'}^{l, \mu}(\omega) = -\hat{\mathcal{V}}_{\mathbf{k}, \mathbf{k}'}^{l, \mu} - \sum_{\mathbf{q}} \hat{\mathcal{V}}_{\mathbf{k}, \mathbf{q}}^{l, \mu} \hat{G}_{\mathbf{q}}^0(\omega) \hat{T}_{\mathbf{q}, \mathbf{k}'}^{l, \mu}(\omega)$ , with  $l = A(B)$ , partial waves are restricted to in-plane  $\mu = s, p_\sigma, d$  harmonics and  $\hat{G}_{\mathbf{q}}^0(\omega)$  is the bare Green's function. The  $T$ -matrix equations can be solved and the subsequent averaging over random distribution of impurities transforms  $T$ -matrix into the spin-wave self-energies  $\hat{\Sigma}_{\mathbf{k}}(\omega) = x \delta_{\mathbf{k}-\mathbf{k}'} \sum_{\mu} \left[ \hat{T}_{\mathbf{k}, \mathbf{k}'}^{A, \mu}(\omega) + \hat{T}_{\mathbf{k}, \mathbf{k}'}^{B, \mu}(\omega) \right]$ . Summation

of the Dyson-Belyaev diagrammatic series for the Green's functions gives  $\hat{G} = \hat{G}^0 + \hat{G}^0 \hat{\Sigma} \hat{G}$  and then the transverse component of the neutron scattering dynamical structure factor is proportional to the linear combination of the spectral functions

$$\mathcal{S}^\perp(\mathbf{k}, \omega) = f(\mathbf{k})g(\omega) [A_{\mathbf{k}}^{11}(\omega) + A_{\mathbf{k}}^{22}(\omega) + 2A_{\mathbf{k}}^{12}(\omega)] ,$$

where  $A_{\mathbf{k}}^{ij}(\omega) = -\frac{1}{\pi} \text{Im} \hat{G}_{\mathbf{k}}^{ij}(\omega)$ , kinematic form-factor  $f(\mathbf{k}) = \pi S(1 - \gamma_{\mathbf{k}})/\omega_{\mathbf{k}}$ ,  $g(\omega) = [1 + n_B(\omega)] = [e^{\omega/T} - 1]^{-1}$  is the Bose distribution function.

The static properties of the system are calculated from the spin-wave expression of the averaged on-site magnetic moment:

$$|\langle S_i^z \rangle| = S + \frac{1}{2} - \sum_{\mathbf{k}} \frac{1}{\omega_{\mathbf{k}}} \left[ \frac{1}{2} + \langle \alpha_{\mathbf{k}}^\dagger \alpha_{\mathbf{k}} \rangle - \gamma_{\mathbf{k}} \langle \alpha_{\mathbf{k}}^\dagger \beta_{\mathbf{k}}^\dagger \rangle \right] ,$$

where bosonic averages can be expressed through the spectral functions.

## II. RESULTS

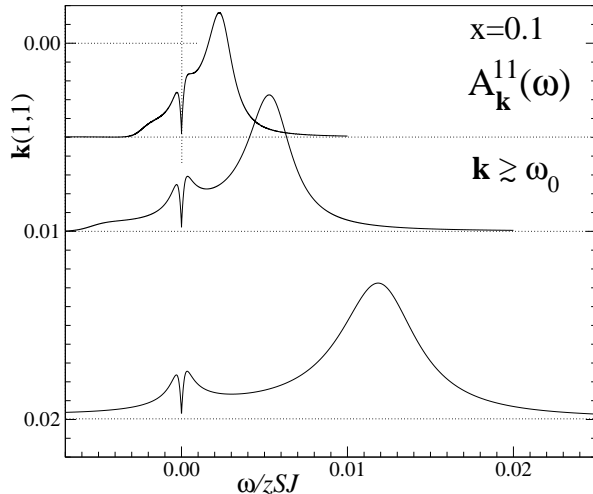


FIG. 1. The spectral function  $A_{\mathbf{k}}^{11}(\omega)$  for the wave-vectors  $\mathbf{k} = 0.005, 0.01$ , and  $0.02$  along the  $(1, 1)$  direction,  $\mathbf{k} = 0.005$  is of the order of  $\omega_0$ .  $A_{\mathbf{k}}^{11}(\omega)$  for each  $\mathbf{k}$  is normalized to fit the picture.

A detailed analysis of the spectral function gives the following picture. At the wave-vectors much larger than  $\omega_0$  ( $\omega_{\mathbf{k}} \gg \omega_0$ ), that is at the wavelengths shorter than a characteristic length  $\ell \sim e^{-\pi/4x}$ , the spectral function has three distinct regions in  $\omega$ . First, is a vicinity of a quasiparticle peak,  $\omega \approx \tilde{\omega}_{\mathbf{k}}$ , where the spectrum has a regular Lorentzian form with the pole at  $\tilde{\omega}_{\mathbf{k}}$  and width  $\tilde{\gamma}_{\mathbf{k}}$  given by the perturbative result. Second, the intermediate range of energies,  $\omega_0 < \omega \ll \tilde{\omega}_{\mathbf{k}}$ , where the spectral function is independent of  $\omega$  and corresponds to an almost flat, shallow ( $\sim x$ ) background of states. Third, the

vicinity of a “localization peak”,  $\omega \approx \omega_0$ , where the spectral function rises sharply from the shallow background states  $\sim x$  to a peak of the height  $\sim 1/x$  and then vanishes in a singular fashion as  $\omega$  approaches zero. The spectral function  $A_{\mathbf{k}}^{11}(\omega)$  is shown in Fig. 1 for a representative value of impurity concentration  $x = 0.1$ . One can clearly see the features we have discussed above: the broadened quasiparticle peak, the localization peak, and the states between them. As the  $\mathbf{k}$  decreases all the mentioned structures merge.

The average on-site magnetic moment for randomly diluted AF with the averaging over magnetic sites  $M(x) = \sum_i |S_i^z|/N_m$  can be expressed through the integral of the spectral functions as:

$$M(x, T) = S - \Delta - \delta M(x, T) , \quad (4)$$

$$\delta M(x, T) = \sum_{\mathbf{k}} \int_{-\infty}^{\infty} \frac{n_B(\omega) d\omega}{\omega_{\mathbf{k}}} [A_{R, \mathbf{k}}^{11}(\omega) - \gamma_{\mathbf{k}} A_{R, \mathbf{k}}^{12}(\omega)] ,$$

where  $\Delta = \sum_{\mathbf{k}} v_{\mathbf{k}}^2 \simeq 0.1966$  is the zero-point spin deviation, subscript  $R$  denotes retarded.

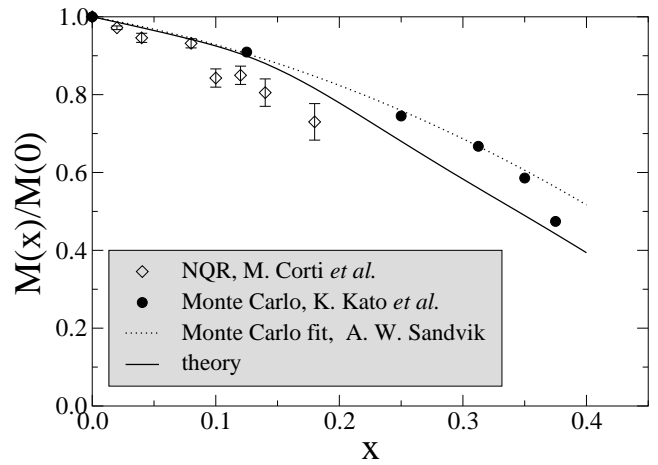


FIG. 2. Average staggered magnetization v.s.  $x$ . Our results from Eq. (4) (solid line), Monte Carlo data (circles, Ref. [9]), NQR data (diamonds, Ref. [15]), and the fit of Monte Carlo data from Ref. [10] (dotted line) are shown.

Numerical integration of the expression in Eq. (4) gives the suppression rate of the staggered magnetization  $M(x) \simeq M(0) - Bx$  with  $B = 0.209(8)$ . For  $S = 1/2$  it gives the slope of the normalized staggered magnetization  $M(x)/M(0) \simeq 1 - Bx/(S - \Delta) \simeq 1 - 0.691(5) \cdot x$ . The staggered magnetization v.s.  $x$  is presented in Fig. 2 for  $S = 1/2$ . The recent Monte Carlo data Refs. [9,10], and NQR data Ref. [15] are also shown. One can see a very good agreement of our results with numerical data up to high concentrations.

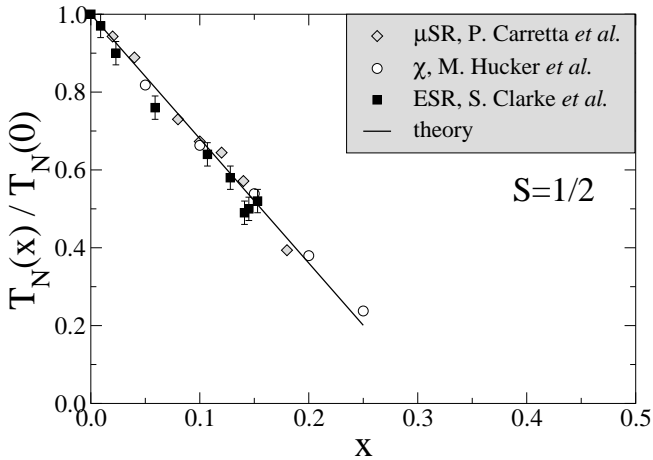


FIG. 3.  $T_N(x)/T_N(0)$  v.s.  $x$  for  $S = 1/2$ . Our results (solid line),  $\mu$ SR (diamonds) [7], magnetic susceptibility (circles) [6], and ESR (squares) [8] data.

At  $T > 0$  the staggered magnetic moment consists of the quantum,  $T = 0$ , and thermal,  $T$ -dependent, parts. For the true 2D system at  $x = 0$  and  $T > 0$  thermal fluctuation destroy the long-range order which manifests itself as a log-divergency of the thermal correction to the magnetization. The 3D coupling provides a cut-off to this divergency in a quasi-2D problem which yields the finite value of the thermal correction and the finite value of the Néel temperature whose mean-field value can be found from the condition  $M(x, T_N) = 0 = S - \Delta - \delta M(x, T_N)$ . Suppression rate of the Néel temperature can be readily obtained  $\frac{T_N(x)}{T_N(0)} \simeq 1 - A_s x = 1 - x \left( \pi - \frac{2}{\pi} + \frac{B}{S-\Delta} \right)$ . For  $S = 1/2$  this gives  $A_{1/2} = 3.196(5)$  and for  $S = 5/2$  it is  $A_{5/2} = 2.600(4)$ . We plot our results for  $T_N(x)/T_N(0)$  for the case of  $S = 1/2$  in Fig. 3 together with experimental data. One can see that our results agree very well with the experiments up to a rather high doping level  $x \approx 0.25$ .

### III. CONCLUSIONS

We have studied the problem of diluted 2D and quasi-2D quantum Heisenberg antiferromagnets in a tetragonal lattice making use of linear spin-wave theory and  $T$ -matrix approach. We have shown that the spin-wave spectrum is strongly modified by disorder which indicates magnon localization on a length scale  $\ell$ , exponentially large in  $1/x$ . This new length-scale appears explicitly in the dynamic properties such as the dynamical structure factor  $\mathcal{S}(\mathbf{k}, \omega)$  which can be measured directly in neutron scattering experiments, and the magnon density of states  $N(\omega)$ , which is directly related to the magnetic specific heat. The measurement of such quantities will provide a direct test of our theory. Furthermore, we show that the static properties such as the zero-temperature staggered magnetization and Néel temperature do not show

any anomaly associated with the spectrum and are finite up to the concentration close to the classical percolation threshold. These results are in a quantitative agreement with the NQR,  $\mu$ SR, ESR, and magnetic susceptibility measurements in different compounds as well as with the Monte Carlo data. Thus, in low-dimensional systems with disorder the connection between static and dynamic quantities is not straightforward. Altogether this provides a self-consistent picture of the effects of disorder in low-dimensional quantum antiferromagnets.

### ACKNOWLEDGMENTS

This research was supported in part by Oak Ridge National Laboratory, managed by UT-Battelle, LLC, for the U.S. Department of Energy under contract DE-AC05-00OR22725, and by a CULAR research grant under the auspices of the US Department of Energy.

- 
- <sup>†</sup> Also at the Institute of Semiconductor Physics, Novosibirsk, Russia.
- <sup>\*</sup> On leave from Department of Physics, University of California, Riverside, CA, 92521.
- [1] N. Nagaosa *et al.*, J. Phys. Soc. Japan **65**, 3724 (1996).
  - [2] V. Yu. Irkhin *et al.*, Phys. Rev. B **60**, 14779 (1999).
  - [3] A. W. Sandvik *et al.*, Phys. Rev. B **56**, 11701 (1997).
  - [4] W. Brenig and A. P. Kampf, Phys. Rev. B **43**, 12914 (1991).
  - [5] S-W. Cheong *et al.*, Phys. Rev. B **44**, R9739 (1991).
  - [6] M. Hücker *et al.*, Phys. Rev. B **59**, R725 (1999).
  - [7] P. Carretta *et al.*, Phys. Rev. B **55**, 3734 (1997).
  - [8] S. J. Clarke and A. Harrison, J. Phys.: Condens. Matter, **4**, 6217 (1992).
  - [9] K. Kato *et al.*, Phys. Rev. Lett. **84**, 4204 (2000).
  - [10] A. W. Sandvik (preprint).
  - [11] A. B. Harris and S. Kirkpatrick, Phys. Rev. B **16**, 542 (1977).
  - [12] R. B. Stinchcombe, in *Phase Transitions and Critical Phenomena* (Academic Press, London, 1983), Vol. 7; R. A. Tahir-Kheli, *ibid.*, Vol. 5B, p. 259.
  - [13] C. C. Wan *et al.*, Phys. Rev. B **48**, 1036 (1993).
  - [14] A. L. Chernyshev *et al.*, Phys. Rev. Lett **87**, 067209 (2001).
  - [15] M. Corti *et al.*, Phys. Rev. B **52**, 4226 (1995).